Osmotic mass transfer through a cylindric semipermeable membrane

Larisa Beilina

January 8, 1999

Abstract

We consider capillary and diffusion models of water transfer through semi-permeable membranes as a problem with free boundary in the case of axi-symmetry. The problems are solved using an adaptive mixed finite element method based on an a posteriori error estimate.

Acknowledgements

I am deeply indebted to Claes Johnson, my supervisor, for constant support and encouragement in my research. To work with him has been an enriching experience for me. I want to thank Mårten Levenstam for his comments and advices regarding this work. I gratefully acknowledge the financial support from the Swedish Institute. I also want to thank Vadim Beilin for helpful discussions. I would like to acknowledge the constant support and loving care that I have received from my dear family, Ilya and Alesha, as well as my mother, J.G.Krotova.

Contents

1 Introduction

Mass transfer through a semipermeable membrane plays a central role in biology and particularly in cytology, physiology and botany. Membranes separate and organise the cell and allow exchange with the environment. The concentration of solutes varies inside and outside the cell. Without a membrane solutes would move by diffusion down their concentration gradients, and membranes restrict this movement.

Many biological membranes do not restrict the movement of water to the same extent as solutes. Water moves across membranes toward the region of highest total solute concentration. We shall consider osmosis, that is movement of water across membranes because of differences in solute concentrations.

Historically the first who considered osmotic pressure was Jean-Antoine Nollet (1700-1770). In 1748 he showed that in two compartments with a semipermeable membrane, which was not permeable to solute, water moves from low to high concentration [7]. The movement stops when the hydrostatic pressure pushes an equal amount of water back to the equilibrium.

The instrument to measure osmotic pressure is called an osmometer. It is a vessel whose walls are permeable by water to a greater extent than another liquid.

The German botanist Wilhelm Pfeffer (1845-1920) made the first quantitative measurements of osmotic pressure in 1877. He coated porous clay cups with ferro-cyanide to make a membrane that allowed water to diffuse freely while sucrose diffused very slowly. The clay cups were rigid and could withstand a pressure. He found that the osmotic pressure was proportional to temperature and to the solute concentration.

The apparently first paper on the dynamic theory of osmotically induced mass transfer through a semipermeable deformable membrane was [9], where the principal relationship between the thermodynamic variables and frictional theory of diffusion was formulated.

Mass transfer through deformable membranes as a class of free boundary problems has not been studied from the mathematical point of view. Moreover, the dynamic nature of osmosis is not fully understood: the two existing approaches—diffusion and capillary models—are concurrently used, although arguments in favour of one or another approach do not exist [11],[10],[2].

In order to obtain a better understanding of the water flow in the capillary model, we shall consider sea urchin eggs, which contain a constant volume in iso-osmotic solution of NaCl, put in CaCl_2 with a solution that is iso-osmotic. The eggs swell and water enters, because membrane is selectively permeable and does not allow Na to pass. However, Ca moves into the cell down its

concentration gradient and water moves from high to low concentration and follows the Ca.

A recent monograph [8] formulates the problem of mass transfer in a common osmometer (a narrow tube with a flat semipermeable interface across the tube) as a one dimensional boundary value problem for a differential equation, and numerically solves this problem using a finite difference method.

However, their method essentially uses the one-dimensional character of the problem, and cannot be easily extended to model biological cells. The reason is that in a one-dimensional case an incompressible liquid moves as a whole, so its velocity depends on time only and not on the space coordinate.

In this paper we demonstrate that corresponding problems in three dimensions assuming cylindrical symmetry, can be solved using a finite element method. We consider two essentially different models, a capillary model and a diffusion model. In the capillary model, the membrane is filled with water, whose motion is governed by Darcy's law. In the diffusion model, the membrane is a layer of solute, governed by the Navier-Stokes equations. In the mathematical models we assume that the walls are strictly semipermeable, that is the solute cannot penetrate them even in small quantities.

The problem of osmotically induced mass transfer in an osmometer open through a manometric tube, is formulated as a free boundary value problem. We solve numerically both the existing models of osmosis and compare the results of the simulations.

An outline of the paper is as follows: in Section 2 we consider mathematical models for capillary and diffusion models in the form of systems combining the Navier-Stokes equations, Darcy's law and concentration equations in the setting of free boundary problems in the case of axi-symmetry. In Section 3.1 we present a finite element method for solving Navier-Stokes equations, Darcy's law and concentration equations. In Section 3.2 considered the dual problem to the Navier-Stokes equation and an a posteriori error estimate. In Section 3.4 we present numerical results and compare the capillary and diffusion models.

2 The mathematical model.

We consider a cylindrical osmometer, immersed in a water basin, as depicted in Figure 1. Let (r, z, φ) denote cylindrical coordinates and t time. The problem is analysed using a capillary model and a diffusion model. The main difference between these two cases is the way the membrane is modelled. In the capillary model we consider the membrane as a thin semipermeable layer filled with pure water. In the diffusion model the membrane is a perfect diluted water solution of the same liquid component, bounded by a infinitely thin two-sided non-deformable semipermeable layer.

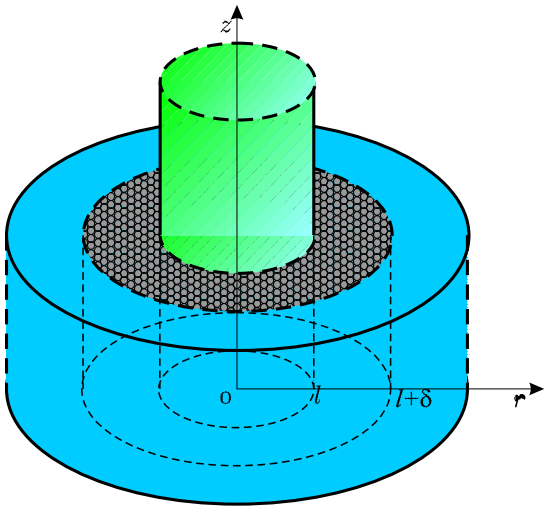

Figure 1: An open osmometer bounded by a rigid porous semipermeable membrane

We assume the solution to be axi-symmetric, that is, independent of the azimuthal coordinate φ.

We assume that mechanical and thermodynamic equilibrium is attained instantaneously at the membrane boundaries.

In the paper we will use the following notation:

- $c(r, z, t)$ — volume concentration of the water,
- $v(r, z, t)$ — the average volume velocity of the water,
- $p(r, z, t)$ — pressure of the water.

We also assume that the pressure p at the open end of the manometric tube is equal to zero.

2.1 Capillary model.

In the capillary model, we will consider four regions, depicted in Figure 2:

$$\begin{aligned} Vol_0 &= \{(r,z):\ z>h, r<l_1\}, \\ Vol_1 &= \{(r,z):\ z<h, r<l_1\}, \\ Vol_2 &= \{(r,z):\ z<h, l_1<r<l_2\}, \\ Vol_3 &= \{(r,z):\ z<h, r>l_2\}. \end{aligned} \tag{1}$$

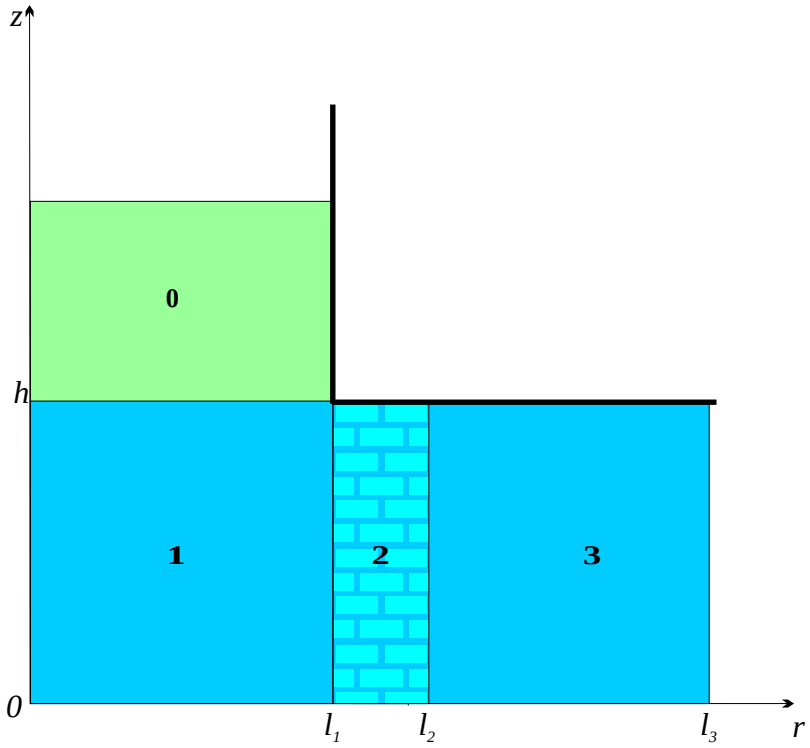

Figure 2: Volumes in the capillary model

We assume that Vol_0 and Vol_1 are filled with a perfect mixture of water W and an incompressible liquid component A with a constant nonzero initial concentration of both components. We assume that A does not penetrate into Vol_2, and the porous space of the membrane Vol_2 and the water basin Vol_3 are filled with pure water. Further, we assume that the process under consideration is isothermal and that the density ρ of the impermeant A and that of the water coincide and are equal to 1.

If necessary, we will use additional indices for the volume and coordinate axis. For example, $v_{r,\,Vol_3}$ is the r-component of velocity in the Vol_3.

2.1.1 Governing equations

Equation of state, expressing the additivity of volumes:

$$c_{Vol_i} + c^A_{Vol_i} = 1, \quad i = 0, 1, 2, 3, \tag{2}$$

where c^A is the volume concentration of component A.
Equation of continuity:

$$\text{div } \vec{v}_{Vol_i} = 0, \quad i = 0, 1, 2, 3. \tag{3}$$

or, in cylindrical coordinates :

$$\text{div } \vec{v}_{Vol_i} = \frac{1}{r}\frac{\partial}{\partial r}(r v_{r,\,Vol_i}) + \frac{1}{r}\frac{\partial}{\partial \varphi}(v_{\varphi,\,Vol_i}) + \frac{\partial}{\partial z}(v_{z,\,Vol_i}) = 0 \tag{4}$$

which in the case of axi-symmetry amounts to

$$\frac{1}{r}\frac{\partial}{\partial r}(r v_{r,\,Vol_i}) + \frac{\partial}{\partial z}(v_{z,\,Vol_i}) = 0. \tag{5}$$

Equation of convection-diffusion transfer of the water:

$$\frac{\partial c_{Vol_i}}{\partial t} + \nabla \cdot (v_{Vol_i} c_{Vol_i}) - D\Delta c_{Vol_i} \;=\; 0, \qquad i = 0, 1, \tag{6}$$

where D is the diffusion coefficient.

Using the facts that

$$\nabla \cdot (vc) = (\nabla c) \cdot v + c(\nabla \cdot v)$$

and $\nabla \cdot v_{Vol_i} = 0$, we have

$$\nabla \cdot (v_{Voli} c_{Vol_i}) = (\nabla c_{Vol_i}) \cdot v_{Vol_i}, \tag{7}$$

and thus the *equation of convection-diffusion* transfer in the case of axi-symmetry can be written:

$$\frac{\partial c_{Vol_i}}{\partial t} + (\nabla c_{Vol_i}) \cdot v_{Vol_i} - D\Delta c_{Vol_i} \;=\; 0, \tag{8}$$
$$\text{for } t > 0 \text{ and } i = 0, 1.$$

In cylindrical coordinates in the case of axi-symmetry this equation takes the form:

$$\frac{\partial c_{Vol_i}}{\partial t} + \frac{\partial c_{Vol_i}}{\partial r} \cdot v_{r\,Vol_i} + \frac{\partial c_{Vol_i}}{\partial z} \cdot v_{z\,Vol_i} - D\left(\frac{\partial^2 c_{Vol_i}}{\partial r^2} + \frac{1}{r}\frac{\partial c_{Vol_i}}{\partial r} + \frac{\partial^2 c_{Vol_i}}{\partial z^2}\right) = 0. \tag{9}$$

Equation of motion of the solution (Navier-Stokes equation):

$$\frac{\partial v_{Vol_i}}{\partial t} + (v_{Vol_i} \cdot \nabla) v_{Vol_i} - \mu \cdot \triangle v_{Vol_i} = -\frac{1}{\rho} \nabla p_{Vol_i}, \quad i = 0, 1, 2, 3,$$

where μ is the viscosity and ρ is density of the water. In cylindrical coordinates in the case of axi-symmetry this equation takes the form:

$$\begin{aligned}
\frac{\partial v_{r\,Vol_i}}{\partial t} + v_{r\,Vol_i} \frac{\partial v_{r\,Vol_i}}{\partial r} + v_{z\,Vol_i} \frac{\partial v_{r\,Vol_i}}{\partial z} - \mu \cdot \triangle v_{r\,Vol_i} + \frac{1}{\rho} \frac{\partial p_{Vol_i}}{\partial r} &= 0, \\
\frac{\partial v_{z\,Vol_i}}{\partial t} + v_{r\,Vol_i} \frac{\partial v_{z\,Vol_i}}{\partial r} + v_{z\,Vol_i} \frac{\partial v_{z\,Vol_i}}{\partial z} - \mu \cdot \triangle v_{z\,Vol_i} + \frac{1}{\rho} \frac{\partial p_{Vol_i}}{\partial z} &= 0.
\end{aligned}$$

Darcy's law, describing the water percolation through the membrane:

$$v_{Vol_2} = -k \nabla p_{Vol_2},$$

where k is the percolation coefficient through the membrane, which in cylindrical coordinates in the case of the axi-symmetry reads:

$$\begin{aligned}
v_{r\,Vol_2} &= -k \frac{\partial p_{Vol_2}}{\partial r}, \\
v_{z\,Vol_2} &= -k \frac{\partial p_{Vol_2}}{\partial z}.
\end{aligned}$$

2.1.2 Initial and boundary conditions

Since the porous space of the membrane saturated by pure water, there is no osmotically induced pressure jump. This fact and the continuity of the water flux yield the following interior boundary conditions:

$$\begin{aligned}
v_r(l_1-, t) &= v_r(l_1+, t), \\
v_z(l_1-, t) &= v_z(l_1+, t), \\
p(l_1-, t) &= p(l_1+, t), \\
v_r(l_2-, t) &= v_r(l_2+, t), \\
v_z(l_2-, t) &= v_z(l_2+, t), \\
p(l_2-, t) &= p(l_2+, t), \\
\text{for any } t &\geq 0.
\end{aligned}$$

Since only water saturates the porous space of the membrane, we have the following boundary condition for the concentration :

$$c(l_1, t) = 1. \tag{10}$$

2.2 Diffusion model.

The membrane is modelled as a perfect diluted water solution of a liquid impermeant B with a constant nonzero initial concentration of both components saturating region Vol_3 and bounded by the infinitely thin two-sided non-deformable semipermeable surface Vol_2 and Vol_4, impermeable to B. The volumes are depicted in Figure 3. Note, that volume numbers have been changed.

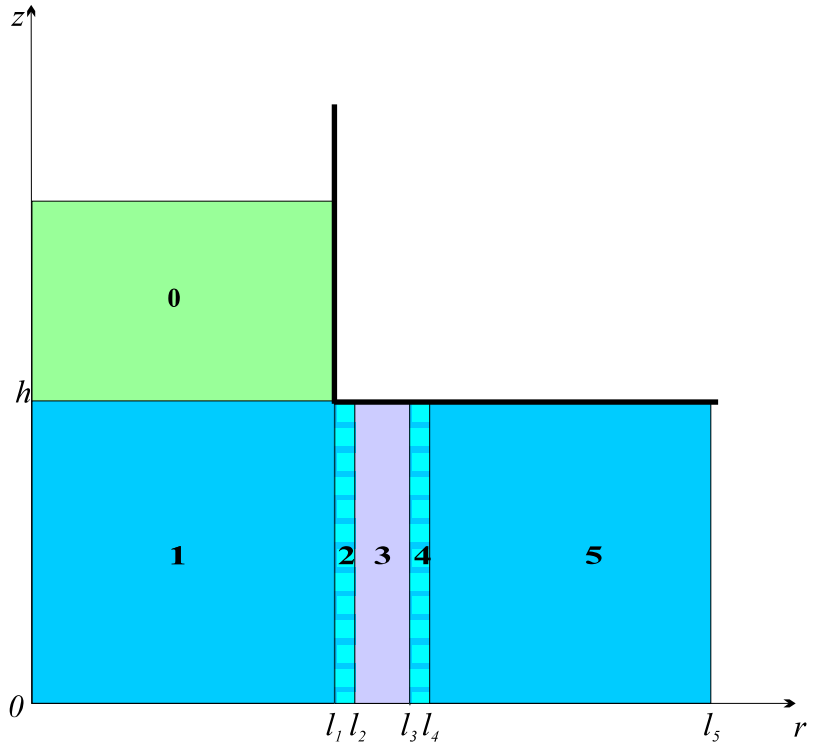

Figure 3: Scheme of an open osmometer in diffusion model

As in the previous case assume, that Vol_0 and Vol_1 are filled with a perfect mixture of water and an incompressible liquid component A with a constant nonzero initial concentration of both components. Assume that A does not penetrate into Vol_2 and that the infinitely thin two-sided non-deformable semipermeable surface Vol_2, Vol_4 and the water basin Vol_5 are filled with pure water. Assume that the densities of the impermeant A in the osmometer and the impermeant B in the membrane are equal to the density of water.

To describe this model mathematically we need to replace *Darcy's law*,

which models the water flow in the capillary model, by the *Navier-Stokes equation* in the diffusion model inside the membrane or in region Vol_3. We now denote by v_{Vol_3} the average volume velocity of the solution inside the membrane. To determine the concentration distribution in region Vol_3, we use a *convection-diffusion equation.*

Assume, that there is friction between the solution representing the membrane and some infinitely thin rigid solid, connecting the fixed membrane boundaries $r = l_1$ and $r = l_4$, and the solution saturating the membrane moves according to *Darcy's law.*

2.2.1 Governing equations

Now the equations that describe the process of water transfer through the rigid semipermeable membrane are :
Equation of state, expressing the additivity of volumes in Vol_3:

$$c + c^B = 1, \tag{11}$$

where c^B is the volume concentration of component B.
Equation of convection-diffusion transfer of B and W in Vol_3 :

$$\frac{\partial c}{\partial t} + \nabla \cdot (vc) - D\Delta c = 0,$$

where D is the diffusion coefficient.
Equation of continuity in volumes Vol_2, Vol_3, Vol_4:

$$\operatorname{div} \vec{v} = 0. \tag{12}$$

Equation of motion of the solution inside membrane in Vol_3: (Navier-Stokes equation):

$$\frac{\partial v}{\partial t} + (v \cdot \nabla)v - \mu \cdot \triangle v = -\frac{1}{\rho}\nabla p, \tag{13}$$

where μ is viscosity and ρ is density of the water.
Darcy's law, describing the water percolation in volumes Vol_2, Vol_4:

$$v = -k\nabla p.$$

All the other equations for the osmometer, osmotic tube and water basin are the same as for other model.

2.2.2 Initial and boundary conditions

Since the porous space of the membrane is saturated by pure water, there is no osmotically induced pressure jump. This fact and the continuity of the water flux yield the following interior boundary conditions:

$$\begin{aligned}
v_r(l_2-,t) &= v_r(l_2+,t),\\
v_z(l_2-,t) &= v_z(l_2+,t),\\
p(l_2-,t) &= p(l_2+,t),\\
v_r(l_3-,t) &= v_r(l_3+,t),\\
v_z(l_3-,t) &= v_z(l_3+,t),\\
p(l_3-,t) &= p(l_3+,t),\\
v_r(l_4-,t) &= v_r(l_4+,t),\\
v_z(l_4-,t) &= v_z(l_4+,t),\\
p(l_4-,t) &= p(l_4+,t),\\
v_r(l_1-,t) &= v_r(l_1+,t),\\
v_z(l_1-,t) &= v_z(l_1+,t),\\
p(l_1-,t) &= p(l_1+,t),\\
\text{for any } t &\geq 0.
\end{aligned}$$

Since only water saturates infinitely thin two-sided non-deformable semipermeable surfaces Vol_2, Vol_4 of the membrane, we have the following boundary conditions for the concentration:

$$c(l_3,t) = 1, \tag{14}$$
$$c(l_2,t) = 1, \tag{15}$$
$$c(l_3,t) = 1. \tag{16}$$

3 Numerical algorithm

3.1 Finite element formulation

Let us consider the capillary model of velocity distribution in the water basin Vol_3, membrane Vol_2, inside cylinder Vol_1 and in the tube Vol_0 and concentration distribution inside cylinder Vol_1 and in the tube Vol_0. In the volumes Vol_0, Vol_1 and Vol_3, we have Navier-Stokes equations and continuity equations, in the volume Vol_2 we have Darcy's law and continuity equations and in the volumes Vol_0, Vol_1 and Vol_3 we have convection-diffusion equation. To meet the condition of incompressibility of the fluid, in the finite element method we use the pressure correction equation

$$\begin{aligned} -\delta \triangle p_{Vol_i} + \nabla \cdot v_{Vol_i} &= 0\ , & (17)\\ \frac{\partial p_{Vol_i}}{\partial n} &= 0 \text{ on } \partial Vol_i, & (18)\\ i &= 0,1,2,3, \end{aligned}$$

where δ is a parameter which we take proportional to the time step τ. The term $-\delta \triangle p$ acts as a stabilisation of the pressure p.

Finally we obtain the following system of equations connecting velocity, concentration and pressure:

$$\begin{aligned} \frac{\partial v_{Vol_i}}{\partial t} + (v_{Vol_i} \cdot \nabla) v_{Vol_i} - \mu \cdot \triangle v_{Vol_i} &= -\frac{1}{\rho} \nabla p_{Vol_i}, & (19)\\ -\delta \triangle p_{Vol_i} + \nabla \cdot v_{Vol_i} &= 0, & (20)\\ i &= 0,1,3\\ v_{Vol_2} &= -k \nabla p_{Vol_2}, & (21)\\ \frac{\partial c_{Vol_i}}{\partial t} + (\nabla c_{Vol_i}) \cdot v_{Vol_i} - D \Delta c_{Vol_i} &= 0, & (22)\\ i &= 0,1, \end{aligned}$$

with boundary conditions $v_{Vol_1} = v_{Vol_2}, p_{Vol_1} = p_{Vol_2}$ at the boundary $r = l_1$, $v_{Vol_3} = v_{Vol_2}, p_{Vol_3} = p_{Vol_2}$ at the boundary $r = l_2$, $v_{Vol_1} = v_{Vol_0}$, $p_{Vol_1} = p_{Vol_0}$ at the boundary tube-sphere, $\frac{\partial p_{Vol_i}}{\partial n} = 0$ on the boundaries of Vol_i, $\frac{\partial v_{Vol_i}}{\partial n} = 0$ on the boundaries of Vol_i, $c(l_1, t) = 1$.

To formulate the finite element method we introduce finite element spaces U_h, Q_h and W_h for the velocity, pressure and concentration, consisting of standard piecewise linear continuous functions on a triangulation T_h and satisfying Dirichlet boundary conditions. We let ${U_h}^0, {Q_h}^0$ and ${W_h}^0$ denote the

corresponding finite element spaces satisfying homogeneous Dirichlet boundary conditions. The finite element method now reads: find (v_h, p_h, c_h) in $U_h \times Q_h \times W_h$ such that

$$\begin{aligned}
(\frac{v^{k+1}_{h\,Vol_i} - v^{k}_{h\,Vol_i}}{\tau} + (v^{k}_{h\,Vol_i} \cdot \nabla) v^{k+1}_{h\,Vol_i} + \frac{1}{\rho}\nabla p^{k+1}_{h\,Vol_i}, u) &= 0, \qquad (23)\\
\forall u \in {U_h}^0, i = 0, 1, 3, & \\
(q, -\delta \triangle p^{k+1}_{h\,Vol_i} + \nabla \cdot v^{k+1}_{h\,Vol_i}) &= 0, \qquad (24)\\
\forall q \in {Q_h}^0, i = 0, 1, 2, 3, & \\
(v^{k+1}_{h\,Vol_2} + k\nabla p^{k+1}_{h\,Vol_2}, u) &= 0, \forall u \in {U_h}^0, \qquad (25)\\
\left(\frac{c^{k+1}_{h\,Vol_i} - c^{k}_{h\,Vol_i}}{\tau} + (\nabla c^{k+1}_{h\,Vol_i}) \cdot v^{k+1}_{h\,Vol_i} - D\Delta c^{k+1}_{h\,Vol_i}, w\right) &= 0, \qquad (26)\\
\forall w \in {W_h}^0, i = 0, 1. &
\end{aligned}$$

3.2 An a posteriori error estimate

In this section we will prove a posteriori error estimate for the incompressible Navier-Stokes equations using the general approach, described in [5],[4]. The proof is based on an error representation in terms of the solution of a linearised dual problem, together with Galerkin orthogonality. The a posteriori error estimates takes the form

$$\|(v - v_h)(T)\| \leq \; SC_i \left(\left\| \frac{h^2}{\mu} \cdot R_1(\widehat{v_h}) \right\| + \|hR_2(v_h)\| \right) \leq \; TOL, \qquad (27)$$

where $\|\cdot\|$ is the L_2 norm, v is the exact velocity, v_h is the computed velocity, $\widehat{v_h} \equiv (v_h, p_h)$ is the computed solution, h is the mesh size, μ is viscosity, $R_1(\widehat{v_h})$ and $R_2(v_h)$ are residuals, C_i is an interpolation constant, S is a stability factor. To obtain the residuals $R_1(\widehat{v_h})$ and $R_2(v_h)$ we insert the computed finite element solution into the differential equation. The interpolation constant depends only on the angles of the computational mesh. The stability factor S is defined by

$$S = \frac{(\int_0^T \|\mu D^2 v_*\| + \|\nabla p_*\|)_{L_2(\Omega)} dt}{\|e(T)\|_{L_2(\Omega)}}, \qquad (28)$$

where (v_*, p_*) is solution of a dual problem with $e(T)$ acting as given data (see 3.3.2).

All quantities for error estimation can be computed. The stability factor is computed by solving the dual problem with an approximation of the data $e(T)$, see [6].

3.3 Proof of the a posteriori error estimate

3.3.1 The dual problem

To prove the a posteriori error estimate we have to estimate the perturbation in the solution due to a perturbation of data. To this end, let (v, p) be the solution of the system

$$\begin{aligned} \frac{\partial v_{Vol_i}}{\partial t} + (v_{Vol_i} \cdot \nabla) v_{Vol_i} - \mu \cdot \triangle v_{Vol_i} &= -\nabla p_{Vol_i}, \quad i = 0, 1, 3 && (29) \\ \nabla \cdot v_{Vol_i} &= 0, \quad i = 0, 1, 2, 3 && (30) \\ v_{Vol_2} &= -k \nabla p_{Vol_2}, && (31) \end{aligned}$$

with given boundary data, and let (v_*, p_*) be a perturbation, i.e.

$$(v + v_*, p + p_*)$$

is another solution with perturbed data. Subtracting the system $(29 - 31)$ for (v, p) from the equations for $(v + v_*, p + p_*)$, gives

$$\frac{\partial v_*}{\partial t} + (v \cdot \nabla)\, v_* + (v_* \cdot \nabla)\, v + (v_* \cdot \nabla)\, v_* - \mu \triangle v_* + \nabla p_* = 0 \quad \text{in } Vol_i,\ i = 0, 1, 3, \qquad (32)$$

$$\begin{aligned} \nabla \cdot v_* &= 0 && \text{in } Vol_i,\ i = 0, 1, 2, 3, && (33) \\ v_*(\cdot, 0) &= -k \nabla p_* && \text{in } Vol_2, && (34) \\ v_* &= 0 && \text{on } \partial Vol_i,\ i = 0, 1, 2, 3, && (35) \\ v_*(\cdot, 0) &= v_{0*}(\cdot) && && (36) \end{aligned}$$

Omitting the quadratic term in this equation we get the linearised perturbation equations:

$$\begin{aligned} \frac{\partial v_*}{\partial t} + (v \cdot \nabla)\, v_* + (v_* \cdot \nabla)\, v - \mu \triangle v_* + \nabla p_* &= 0 && \text{in } Vol_i, i = 0, 1, 3, \\ \nabla \cdot v_* &= 0 && \text{in } Vol_i, i = 0, 1, 2, 3, \\ v_*(\cdot, 0) &= -k \nabla p_* && \text{in } Vol_2, \\ v_* &= 0 && \text{on } \partial Vol_i, i = 0, 1, 2, 3, \\ v_*(\cdot, 0) &= v_{0*}(\cdot) \end{aligned}$$

The dual of this problem is the dual problem underlying the a posteriori error estimate, which takes the form

$$
\begin{aligned}
-\frac{\partial v_*}{\partial t} - (v\cdot\nabla)\, v_* + \nabla v_h \cdot v_* - \mu\triangle v_* - \nabla p_* &= 0, \quad \text{in } Vol_i, i{=}0,1,2,3 \qquad (37)\\
\nabla\cdot v_* &= 0, \qquad \text{in } Vol_i, i=0,1,2,3,\\
v_*(\cdot,0) &= -k\nabla p_* \quad \text{in } Vol_2,\\
v_* &= 0 \qquad \text{on } \partial Vol_i, i=0,1,2,3,\\
v_*(\cdot,T) &= e(\cdot,T),
\end{aligned}
$$

where the velocity error $e^T = v^T - {v_h}^T$ at final time T acts as data. This problem can be given the following variational formulation: find $\widehat{v}_* \equiv (v_*, p_*) \in \widehat{V}$ such that

$$
(-\frac{\partial v_*}{\partial t}, u)_{Vol_i} + L(v, v_h; \widehat{u}, \widehat{v}_*) = 0, \qquad \forall \widehat{u} \equiv (u,q) \in \widehat{V}, \qquad (38)
$$

where

$$
\begin{aligned}
L(v, v_h; \widehat{u}, \widehat{v}_*) &= -((v\cdot\nabla)\, v_* - \nabla v_h \cdot v_*, u)_{Vol_i} + (\mu\nabla v_*, \nabla u)_{Vol_i} -\\
&\quad -(\nabla p_*, u)_{Vol_i} + (q, \nabla\cdot v_*)_{Vol_i} + (v_*, u)_{Vol_2} -\\
&\quad - (\nabla p_*, u)_{Vol_2} + (q, \nabla\cdot v_*)_{Vol_2},\\
&\quad i = 0,1,3. \qquad (39)
\end{aligned}
$$

Introducing the functional

$$
\begin{aligned}
A(v; \widehat{w}, \widehat{u}) &= (\mu\nabla w, \nabla u)_{Vol_i} + ((v\cdot\nabla)w, u)_{Vol_i} +\\
&\quad +(\nabla r, u)_{Vol_i} + (q, \nabla\cdot w)_{Vol_i} +\\
&\quad +(w,u)_{Vol_2} - (k\nabla r, u)_{Vol_2} + (q, \nabla\cdot w)_{Vol_2}, \qquad (40)\\
(v,w)_{Vol_i} &= \int_0^T \int_{Vol_i} v\cdot w \; d\,Vol_i dt, \;\; \widehat{w} \equiv (w,r) \in \widehat{V}, i = 0,1,3, \qquad (41)
\end{aligned}
$$

The system $(29-31)$, containing the Navier-Stokes/Darcy equations from the original system, can be given the following variational formulation: find $\widehat{v} \equiv (v,p) \in \widehat{V}$ such that

$$
\begin{aligned}
(v_t, u)_{Vol_i} + A(v; \widehat{v}, \widehat{u}) &= 0, \quad \forall \widehat{u} \equiv (u,q) \in \widehat{V}, i = 0,1,3, \qquad (42)\\
v(\cdot,0) &= v_0. \qquad (43)
\end{aligned}
$$

The corresponding discrete problem can formulated as finding $\widehat{v_h} \equiv (v_h, p_h) \in \widehat{V_h} = V_h \times H_h$ such that

$$
\begin{aligned}
(v_{h_t}, u_h)_{Vol_i} + A(v_h; \widehat{v}_h, \widehat{u}_h) &= 0, \quad \forall \widehat{u}_h \equiv (u_h, q_h) \in \widehat{V}_h, i = 0,1,3, \qquad (44)\\
v_h(\cdot,0) &= v_{h0}. \qquad (45)
\end{aligned}
$$

We define the error $\widehat{e} = (v - v_h, p - p_h) = (e, e_p) \in \widehat{V_h}$ as the difference between the solutions of (42)–(43) and (44)–(45).

3.3.2 An error representation

To obtain an error representation, we shall use following relations:

(1) $L(v, v_h; \widehat{e}, \widehat{v}_*) = A(v; \widehat{v}, \widehat{v}_*) - A(v_h; \widehat{v}_h, \widehat{v}_*)$;

(2) (38) with $\widehat{u} = \widehat{e}$;

(3) $(-\frac{\partial v_*}{\partial t}, e) = -(v_*(\cdot, T), e(\cdot, T)) + (v_*(\cdot, 0), e(\cdot, 0)) + (e_t, v_*)$;

(4) (42) with $\widehat{u} = \widehat{v}_*$;

(5) (44) with $\widehat{u}_h = \widehat{v}_{*h}$;

(6) $e_t = v_t - v_{h_t}, e(0) = v(0) - v_h(0)$, where $\widehat{v}_{*h} \equiv (v_{*h}, p_{*h}) \in \widehat{V_h}$ is an approximation of the dual solution $\widehat{v}_*$.

We have

$$
\begin{aligned}
\|e(\cdot,T)\|^2_{L_2(\Omega)} &= (e(\cdot,T), e(\cdot,T)) \overset{(2)}{=} \\
&= (v_*(\cdot,T), e(\cdot,T)) + (-\frac{\partial v_*}{\partial t}, e) + L(v, v_{hi}; \widehat{e}, \widehat{v}_*) \overset{(1),(3)}{=} \\
&= (v_*(\cdot,0), e(\cdot,0)) + (e_t, v_*) + A(v; \widehat{v}, \widehat{v}_*) - A(v_h; \widehat{v}_h, \widehat{v}_*) \overset{(6)}{=} \\
&= (v_t, v_*) - (v_{h_t}, v_*) + (v_*(\cdot,0), v(\cdot,0)) - (v_*(\cdot,0), v_h(\cdot,0)) + \\
&\quad + A(v; \widehat{v}, \widehat{v}_*) - A(v_h; \widehat{v}_h, \widehat{v}_*) \overset{(4)}{=} \\
&= (v_0, v_*(\cdot,0)) - (v(\cdot,0), v_*(\cdot,0)) - (v_{h_t}, v_*) + \\
&\quad + (v_*(\cdot,0), v(\cdot,0)) - (v_*(\cdot,0), v_h(\cdot,0)) - A(v_h; \widehat{v}_h, \widehat{v}_*) \overset{(5)}{=} \\
&= (v(0), v_*(\cdot,0) - v_h(\cdot,0)) - (v_{h_t}, v_* - v_{*h}) - \\
&\quad - (v_h(\cdot,0), v_*(\cdot,0) - v_{*h}(\cdot,0)) - A(v_h; \widehat{v}_h, \widehat{v}_* - \widehat{v}_{*h}) = \\
&= (v(0) - v_h(\cdot,0), v_*(\cdot,0) - v_h(\cdot,0)) - \\
&\quad - (\frac{\partial v_h}{\partial t} + (v_h \cdot \nabla) v_h - \mu \cdot \triangle v_h + \nabla p_h, v_* - v_{*h})_{Vol_i} - \\
&\quad - (\nabla \cdot v_h, p_* - p_{*h})_{Vol_i} - \\
&\quad - (v_h + k \nabla p_h, v_* - v_{*h})_{Vol_2} - (\nabla \cdot v_h, p_* - p_{*h})_{Vol_2} \leq \\
&\leq SC_i \left(\left\| \frac{h^2}{\mu} \cdot R_1(\widehat{v}_h) \right\|_{L_2(\Omega)} + \|h \cdot R_2(v_h)\|_{L_2(\Omega)} \right),
\end{aligned}
$$

where h is a maximal diameter of the elements in the mesh, μ is viscosity, $R_1(\widehat{v}_h)$ and $R_2(v_h)$ are residuals on K defined as

$$
\begin{aligned}
R_1(\widehat{v}_h) = &\left| \frac{\partial v_h}{\partial t} + (v_h \cdot \nabla) v_h - \mu \cdot \triangle v_h + \nabla p_h \right|_{Vol_i} + \\
&\left| \mu h^{-1} \left[\frac{\partial v_h}{\partial n} \right] \right|_{Vol_i} + |v_h + k \nabla p_h|_{Vol_2}, i = 0, 1, 3,
\end{aligned}
$$

$$
R_2(v_h) = |\nabla \cdot v_h|_{Vol_i}, i = 0, 1, 2, 3,
$$

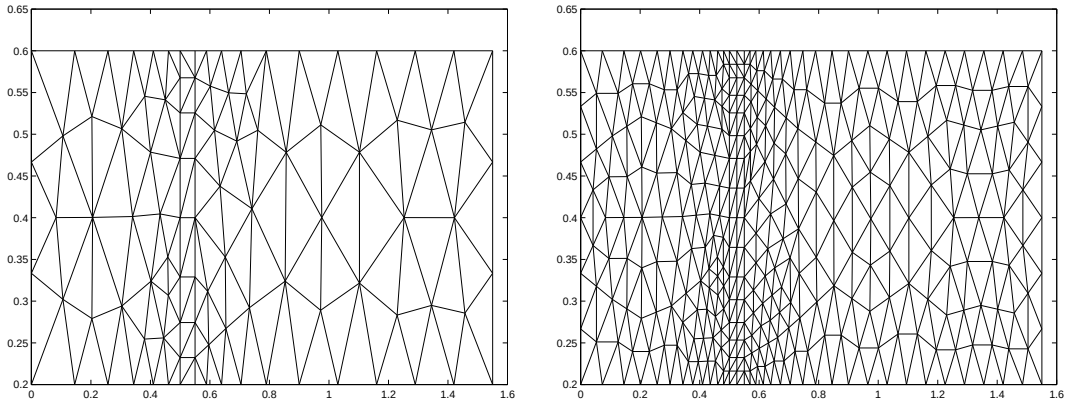

Figure 4: Initial and refined meshes

where $\left[\frac{\partial v_h}{\partial n}\right]$ is the jump in the normal derivative $\frac{\partial v_h}{\partial n}$ across the interior element boundaries, see [5].

3.4 Numerical examples

We performed the computations using MATLAB 5.0, making use of the pdetoolbox for drawing and triangulation. The computation is organised as follows. First we compute a finite element solution $(\widehat{v}_h, c_h)$ an initial coarse mesh T_h and the corresponding residuals $R_1(\widehat{v}_h)$ and $R_2(v_h)$. We then compute a new mesh size h_{new} by seeking to realize $\left\| \frac{h^2}{\mu} \cdot R_1(\widehat{v}_h) \right\|_{L_2(\Omega)} \leq TOL$ with equal error contribution from each element (equidistribution). We repeat this process until satisfaction. For the computation of the stability factor we used fundamental approach. We approximated the solution $(\widehat{v}_h, c_h)$ on the finer mesh and as approximation of the error we used $(\widehat{v}_h, c_h) - (\widehat{v}_{h_{new}}, c_{h_{new}})$. Both meshes and solutions where stored. Then we solved the dual problem on the finer mesh and calculated the second derivative and gradient of the dual solution. Used all the data, we computed the stability factor S with $tau = 0.01$ for 50 time steps. The computed stability factor S was equal to 6.56 for $T = 0.5$. In the time moments $0.2T$ and $0.7T$ we obtained the values $S = 2.94$ and $S = 3.63$ correspondently.

In the Figure 4 we display for the capillary model the initial and final meshes with $TOL = 0.01$, and in Figure 5 we show the velocities for the initial and the final meshes.

The geometry of our domain in our problem is not fixed, since the water level in the vertical tube is changing with time. This means that we cannot use the same mesh in each iteration. Since the tube is narrow, we assume that

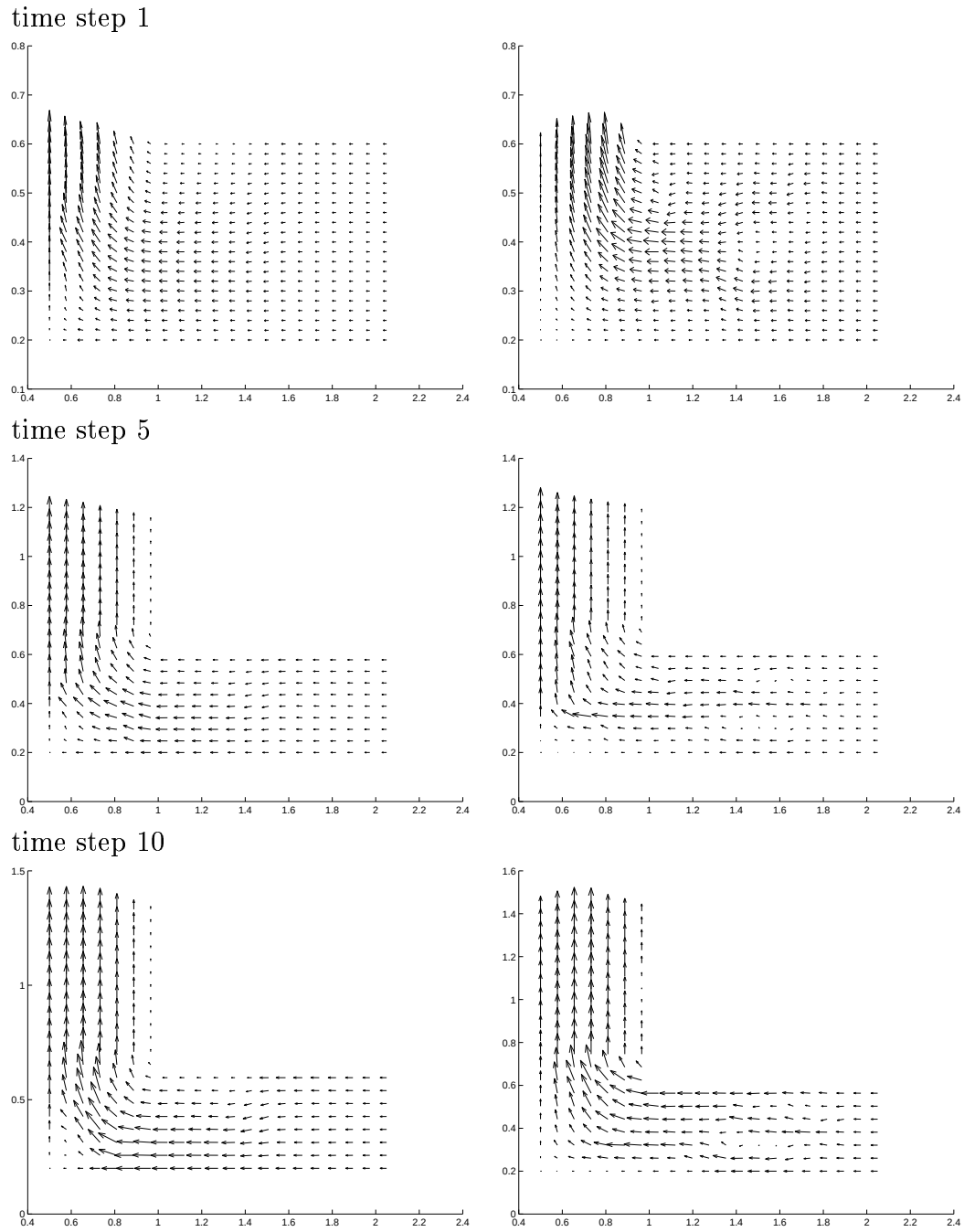

Figure 5: Velocity flow for the original (on the left) and refined (on the right) meshes

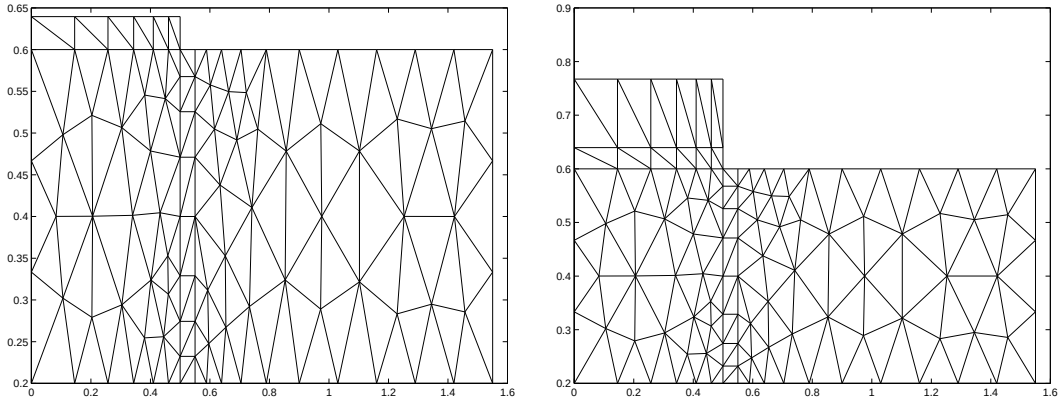

Figure 6: Mesh with moved boundary

the water surface is always horizontal (this assumption is not very realistic, but otherwise the problem would become too complicated). We determine the position of the free boundary by computing in each time step the integral of the flux through the free boundary, and add a new layer to the mesh. Figure 6 shows the initial mesh at time step 2 and 3.

In the actual computations we assume, that the water motion in the membrane is a Poiseuille flow, and the coefficient of the percolation through the membrane is

$$k = \frac{\sigma m}{8\mu}, \tag{46}$$

where m is porosity of the membrane, σ the unit area, μ dynamic viscosity of water. We used the following parameters values:

$$m = 0.02, D = 5 \cdot 10^{-5} cm^2/sec,$$
$$\rho = 1 gr/cm^3, \mu = 0.01 gr/cm \cdot sec.$$

For solving linear system of equations we used Gaussian elimination (see Appendix).

3.4.1 Capillary model

In the computations with the capillary model, we took the initial concentration of the water in the osmometer equal to 0.0002 mol/cm^3 and set the concentration at the boundary of the osmometer-membrane equal to 1. This is because only water saturates the porous space of the membrane. The initial velocity was set equal to zero, because the motion is induced by different concentrations in the membrane and osmometer. The calculations where carried out with the time steps $\tau = 0.01$ for 50 time steps.

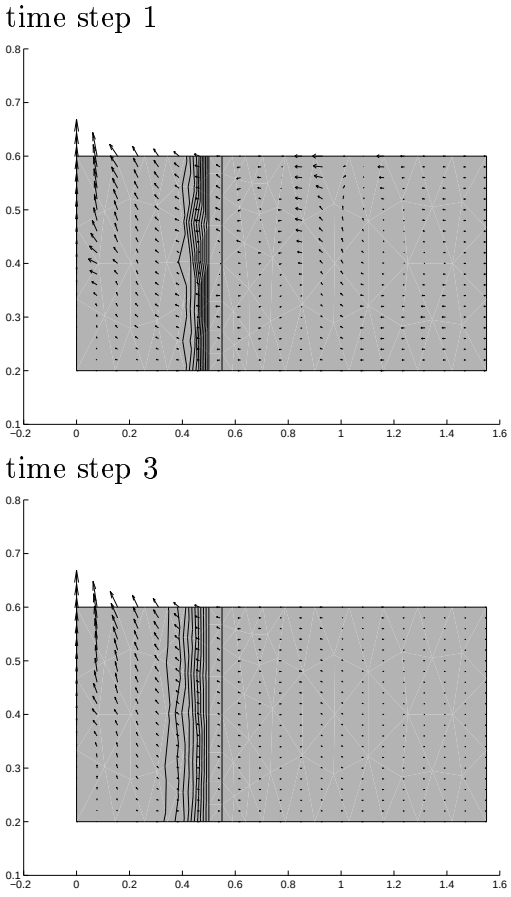

Figure 7: Capillary model of water transfer in the cylinder

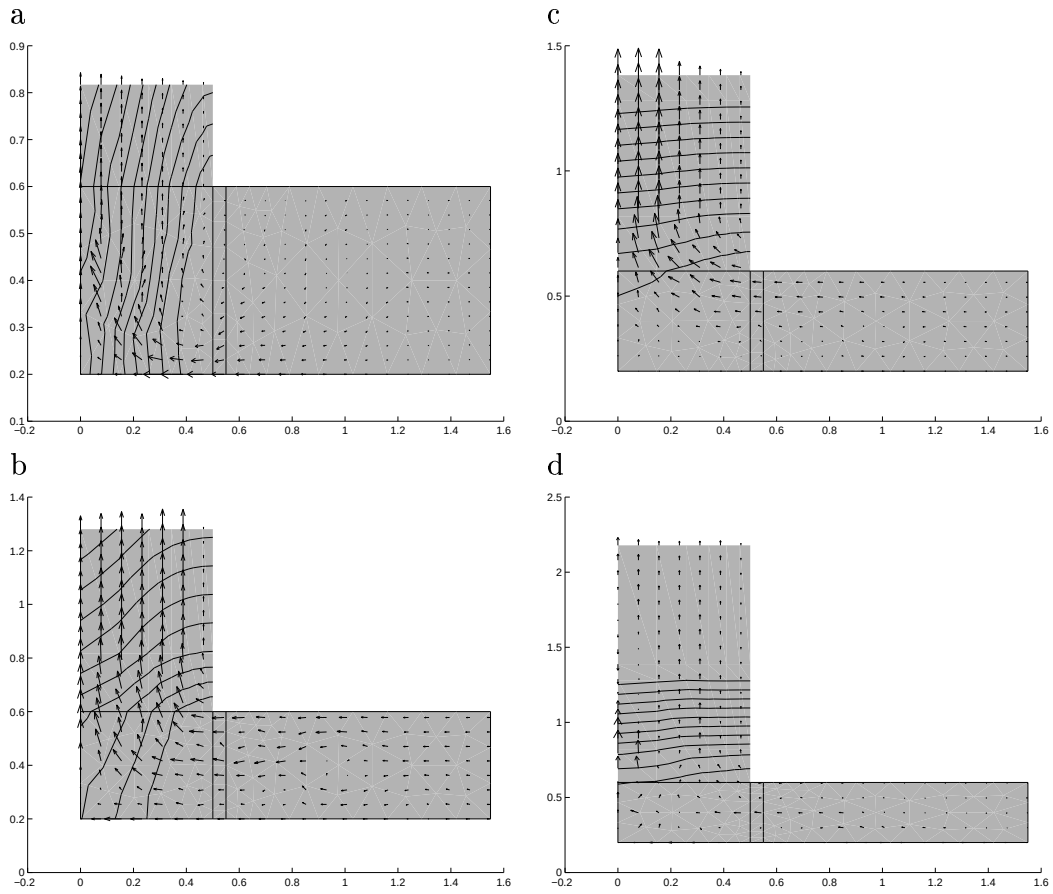

Figure 8: Capillary model of water transfer in the cylinder, 2

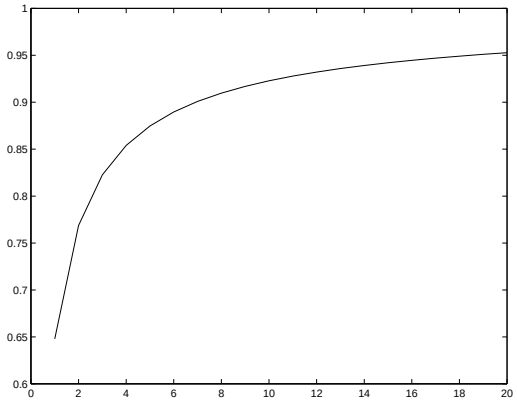

Figure 9: Distribution of the concentration in capillary model in the centre of the cylinder

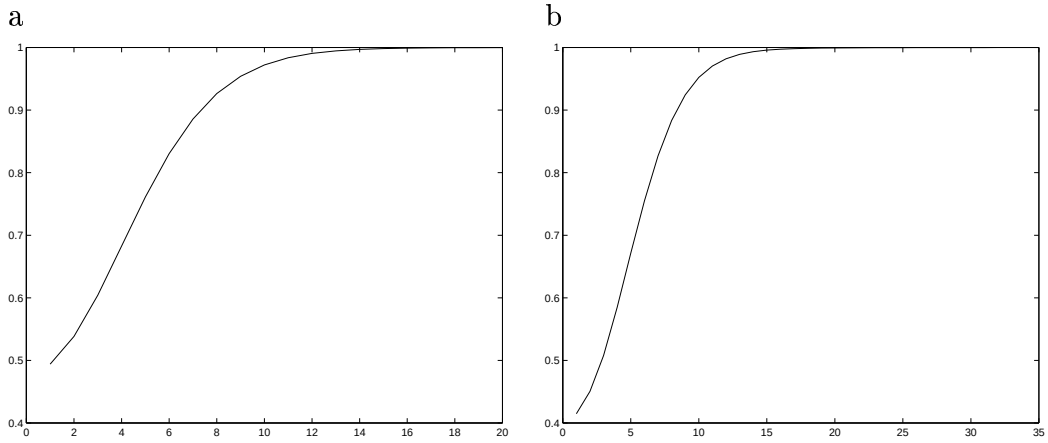

Figure 10: Distribution of the concentration in the osmometer (diffusion model)

Figure 7 shows, that during the first iterations water influx begins and at the membrane boundary and osmometer a diffusion layer appears. The concentration of the water increases faster at the membrane boundary, than at the centre of the cylinder. An intensive water influx through the membrane pushes the liquid out of the osmometer into the vertical tube (see Figure 8a-c). The concentration increases very rapidly at this time moment. After a short time the velocity reaches its maximum (see Figure 8d). The influx stops when the concentration difference across the membrane is balanced by the pressure of the water in the tube, and the velocity decreases to zero. As velocity reaches its maximum the concentration rises to the stationary value (see Figure 9).

3.4.2 Diffusion model

In the diffusion model we assume, that the porous space of the membrane is filled with a perfect mixture of water and some liquid component with nonzero initial concentration, and that the membrane has a very small thickness, and is filled with pure water.

In our calculations we take the initial concentration inside the membrane equal to $0.35 mol/cm^3$ and the initial concentration in the osmometer as in the previous case. The calculations were carried out with the time steps $\tau = 0.1$ for 50 time steps.

In the beginning of the process, water flows through the membrane in the osmometer and pushes the liquid component into the tube (see Figure 11). Because the liquid component cannot be washed from the membrane, inside

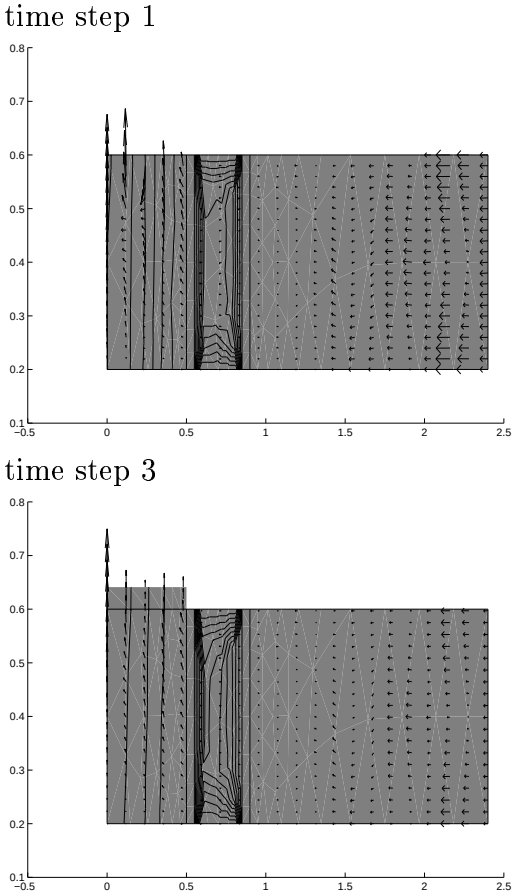

Figure 11: The process of water transfer in diffusion model

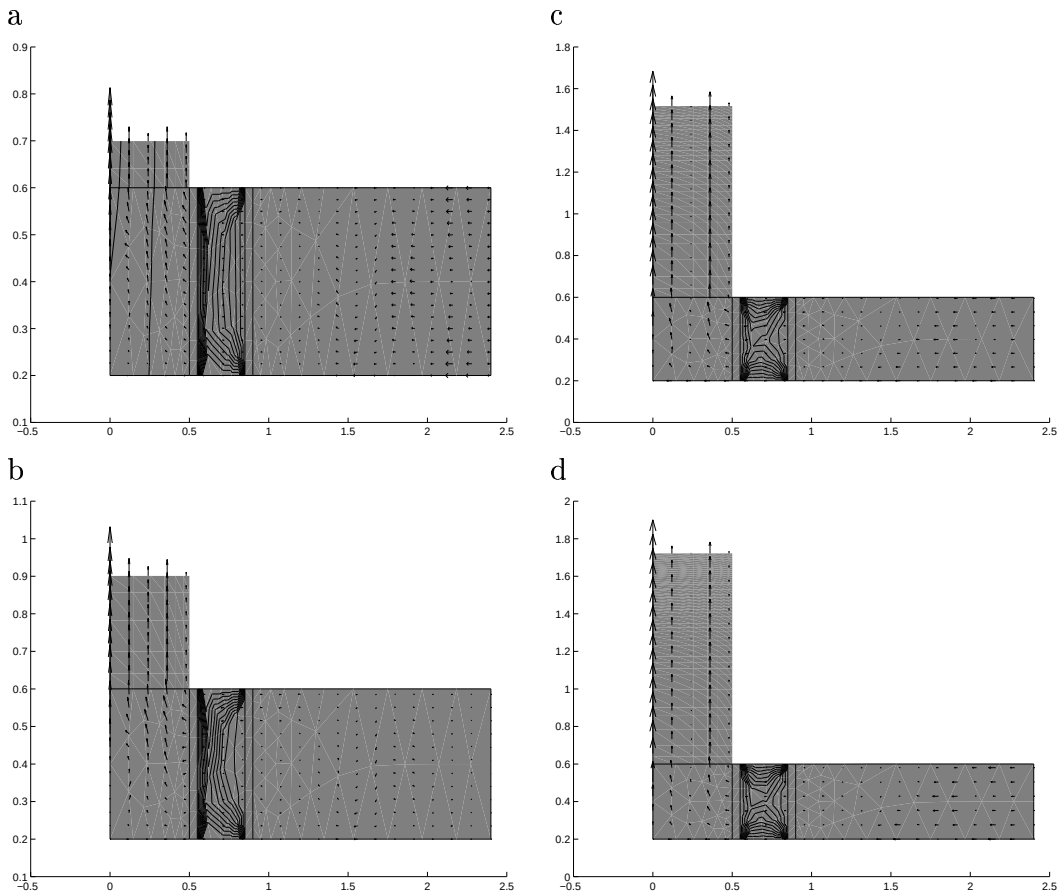

Figure 12: The process of water transfer in diffusion model

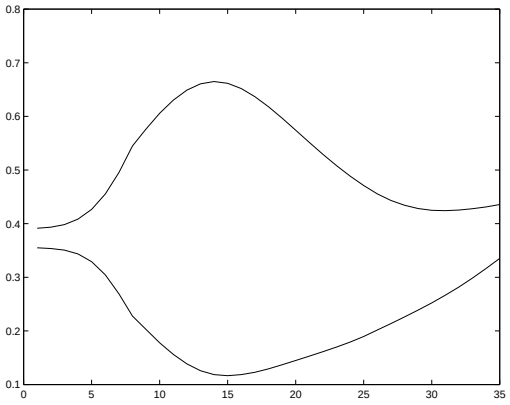

Figure 13: Redistribution of the concentration in diffusion model in membrane

the membrane a redistribution of concentration occurs. In the beginning, water rapidly flows through the membrane and the concentration of the impermeant inside membrane increases at the left border of the membrane. At the other side, the concentration of the liquid component in the osmometer decreases at the border of the membrane, because water goes out to the osmometer and redistributes the solution(see Figure 12). In the Figure 13 we show the concentration inside membrane. The upper figure shows the distribution of the concentration at the left boundary, and the bottom figure shows the distribution of the concentration at the right boundary. In the beginning of the process the concentration at the left boundary inside the membrane begins to increase. At the same time the concentration at the right boundary decreases (see Figure 13). After 15 time steps, when the velocity reaches its maximum and begins to decrease, the concentration inside the membrane redistributes: at the left boundary it decreases and at the right boundary it increases. The concentration from both sides approaches the stationary value after a long time (after 50 time step). The Figure 12 shows how water pushes the liquid into the tube, when the velocity increases. After a short time the velocity reaches its maximum (see Figure 12d). The influx stops and the velocity decreases to zero. At the same time the concentration reaches its stationary value. Figure 10 shows the distribution of the concentration in the osmometer at the down boundary of the osmometer (see Figure 10a)) and at the point at the boundary tube - osmometer (see Figure 10b)).

4 Conclusions

Capillary and diffusion models of water transfer through the semipermeable membrane in the case of axi-symmetry and with a free boundary has been analysed. The problem has been solved using a mixed finite element method. A posteriori error estimate has been considered and used in an adaptive mesh refinement algorithm.

phase	Capillary model	Diffusion model
1	Water flux goes through the membrane into an osmometer and pushes the liquid component into the tube. Velocity and concentration rapidly increase (under 0.02 sec). Near the membrane a diffusion boundary layer is created.	Velocity increases slower (under 0.2 sec) and pushes the liquid component into the tube. The concentration of the water increases in the osmometer and redistributes inside membrane.
2	Velocity reaches its maximum, begins smoothing diffusion in osmometer.	Velocity reaches its maximum, begins smoothing diffusion in osmometer and inside membrane.
3	Velocity decreases until the influx stops, concentration reaches stationary value.	Velocity decreases until the influx stops, concentration reaches stationary value in osmometer and inside membrane.

The calculations show that, qualitatively, the capillary and diffusion models of water transfer through the rigid semipermeable membrane, are indistinguishable.

We can conclude, that both models tend to equilibrium as time tends to infinity. There are no arguments in favour of one or another of these models. This explains why in biophysical literature both these two approaches are used.

References

[1] O.D.Chvolson, Lehrbuch der Physik, Bd 1 Abt 2. Die Lehre von den gasfoermigen, flussigen und festen Korpern. F.Vieweg, Brasunschweig, (1918).

[2] Jack Dainty, Water Relations in Plant Cells. Advanced Bot., Res. I.279-324(1963).

[3] K.Eriksson, D.Estep, P.Hansbo and C.Johnson, Computational Differential Equations. Studentlitteratur, Lund, (1996).

[4] C.Johnson, A.Szepessy, Adaptive finite element methods for conservation laws based on a posteriori error estimates, Comm.pure.appl.-math.48, p.199-234,(1995).

[5] C.Johnson, R.Rannacher and M.Boman, Numerics and hydrodynamic stability: Towards error control in CFD, SIAM J:Numer. Anal. 32, 1058-1079 (1995).

[6] E.Burman, Adaptive finite element methods for compressible two-phase flow. Dep. of Mathematics, Gothenborg, (1998).

[7] J.Nollet, Lectures in experimental philosophy, London:J.Wren, (1792).

[8] L.Rubinstein, B.Martuzans, Free Boundary Problems Related to Osmotic Mass Transfer through semipermeable Membranes, Gakkotosho, Tokyo, (1995).

[9] A.Silberberg, Transport through deformable matrices. Biorheology 26, 291-313 (1989).

[10] W.D.Stein, The Movements of Molekules across Cell Membranes, Academic Press, New York and London, (1967).

[11] J.F.Thain, Principles of Osmotic Phenomena, London, Royal Institute of Chemistry, (1967).

A Appendix

The discrete analogues of the system (24)–(27), taking into account cylindrical coordinates, can be written in matrix form as

$$\begin{aligned}
A1_l v_{ir,l}^{k+1} + B1_l p_{i,l}^{k+1} &= F1_l, \\
A2_l v_{iz,l}^{k+1} + B2_l p_{i,l}^{k+1} &= F2_l, l = 0, 1, 3 \\
A3_l v_{ir,l}^{k+1} + B3_l p_{i,l}^{k+1} &= F3_l, \\
A4_2 v_{ir,2}^{k+1} + B4_2 p_{i,2}^{k+1} &= F4_2, \\
A5_l v_{ir,l}^{k+1} + B5_l v_{iz,l}^{k+1} &= F5_l, l = 0, 1, 2, 3,
\end{aligned}$$

where

$$As = (as_{ij}), Bs = (bs_{ij}), Fs = (fs_1, ..., fs_M), s = 1, ..., 5, \tag{47}$$

$$as_{ij} = \sum_{K \in T_h} as_{ij}^K, bs_{ij} = \sum_{K \in T_h} bs_{ij}^K, fs_i = \sum_{K \in T_h} f_{si}^K,$$

$$\begin{aligned}
a_{1ij}^K &= \frac{1}{\tau} \int\limits_{K_i} \varphi_i \varphi_j r \; dK_i + \sum_{l=1}^{M} v_{ir}^k \int\limits_{K_i} \varphi_l \frac{\partial \varphi_i}{\partial r} \varphi_j r \; dK_i + \\
&\quad + \sum_{l=1}^{M} v_{iz}^k \int \varsigma_l \frac{\partial \varphi_i}{\partial z} \varphi_j r \; dK_i, \\
b_{1ij}^K &= \frac{1}{\rho} \int\limits_{K_i} \frac{\partial \psi_i}{\partial r} \varphi_j r \; dK_i, \\
a_{2ij}^K &= \frac{1}{\tau} \int\limits_{K_i} \varphi_i \varphi_j r \; dK_i + \sum_{l=1}^{M} v_{ir}^k \int \varphi_l \frac{\partial \varphi_i}{\partial r} \varphi_j r \; dK_i + \\
&\quad + \sum_{l=1}^{M} v_{iz}^k \int \varphi_l \frac{\partial \varphi_i}{\partial z} \varphi_j r \; dK_i, \\
b_{2ij}^K &= \frac{1}{\rho} \int\limits_{K_i} \frac{\partial \psi_i}{\partial z} \varphi_j r \; dK_i, \\
a_{3ij}^K &= \int\limits_{K_i} \varphi_i \varphi_j r \; dK_i, \\
b_{3ij}^K &= k \int\limits_{K_i} \frac{\partial \psi_i}{\partial r} \varphi_j r \; dK_i,
\end{aligned}$$

$$
\begin{aligned}
a_{4ij}^K &= \int_{K_i} \varphi_i \varphi_j r \ dK_i, \\
b_{4ij}^K &= k \int\limits_{K_i} \frac{\partial \psi_i}{\partial z} \varphi_j r \ dK_i, \\
a_{5ij}^K &= \int\limits_{K_i} \varphi_i \varphi_j \ dK_i + \int_{K_i} \frac{\partial \phi_i}{\partial r} \phi_j r dK_i, \\
b_{5ij}^K &= \int\limits_{K_i} \frac{\partial \varphi_i}{\partial z} \phi_j r \ dK_i, \\
f_{1i}^K &= v_{ir}^k \frac{1}{\tau} \int\limits_{K_i} \varphi_i \varphi_j r \ dK_i, \\
f_{2i}^K &= v_{iz}^k \frac{1}{\tau} \int\limits_{K_i} \varphi_i \varphi_j r \ dK_i, \\
f_{3i}^K &= 0, f_{4i}^K = 0, f_{5i}^K = 0.
\end{aligned}
$$